

Vortices, Symmetry Breaking, and Temporary Confinement in SU(2) Gauge-Higgs Theory

J. Greensite¹ and Š. Olejník²

¹*Physics and Astronomy Dept., San Francisco State University, San Francisco, CA 94117, USA*

²*Institute of Physics, Slovak Academy of Sciences, SK-845 11 Bratislava, Slovakia*

(Dated: June 14, 2018)

We further investigate center vortex percolation and Coulomb gauge remnant symmetry breaking in the SU(2) gauge-Higgs model. We show that string breaking is visible in Polyakov line correlators on the center projected lattice, that our usual numerical tests successfully relate P-vortices to center vortices, and that vortex removal removes the linear potential, as in the pure gauge theory. This data suggests that global center symmetry is not essential to the vortex confinement mechanism. But we also find that the line of vortex percolation-depercolation transitions, and the line of remnant symmetry breaking transitions, do not coincide in the SU(2)-Higgs phase diagram. This non-uniqueness of transition lines associated with non-local order parameters favors a straightforward interpretation of the Fradkin-Shenker theorem, namely: there is no unambiguous distinction, in the SU(2) gauge-Higgs models, between a “confining” phase and a Higgs phase.

I. INTRODUCTION

Investigations of the confining force generally concentrate on gauge theories in which confinement is permanent; i.e. the linear potential increases without limit. Theories of this kind (with finite rank gauge groups) are all invariant under a global center symmetry, which can be expressed as

$$U_0(\mathbf{x}, t) \rightarrow z U_0(\mathbf{x}, t) \quad \text{all } \mathbf{x}, \text{ fixed } t \quad (1.1)$$

in lattice formulation, where $z \neq 1$ is an element of the (non-trivial) center of the gauge group. The unbroken realization of this symmetry is responsible for the vanishing of Polyakov line expectation values, and hence permanent confinement. For SU(N) gauge theories with this global symmetry, the potential between static color sources, in color group representation r , depends only on the N-ality of representation r . While this fact is easily understood in terms of energetics/string-breaking arguments (e.g. a flux tube between adjoint sources can “snap” due to pair production of gluons), it also means that the string tension of a Wilson loop, evaluated in an ensemble of configurations generated from the pure Yang-Mills action (and therefore blind to the location of the Wilson loop), depends only on the N-ality of the loop representation. This leads to a rather profound conclusion: large-scale vacuum fluctuations – occurring in the *absence* of any external source – must somehow contrive to disorder only the center degrees of freedom of Wilson loop holonomies. The center vortex confinement mechanism (c.f. ref. [1] for a review) is the simplest proposal for how this type of disorder can occur.

However, not all gauge theories of interest are invariant under a non-trivial global center symmetry (1.1). Examples include real QCD, and any other SU(N) gauge theory with matter fields in the fundamental representation of the gauge group. Another relevant example is G(2) pure gauge theory, whose center symmetry and first homotopy group are both trivial.¹ In these theories, the asymptotic string tension is zero,

and at large scales the vacuum state is similar to the Higgs phase of gauge-Higgs theory. Such theories are examples of, rather than exceptions to, the general statement that confinement is dependent on the existence of a non-trivial global center symmetry. On the other hand, real QCD and G(2) pure gauge theory, as well as gauge-Higgs theory in some regions of the phase diagram, have a static quark potential which rises linearly for some interval of color source separation, and then becomes flat. We will refer to this situation as “*temporary confinement*”, reserving the term “*permanent confinement*” for theories which have a non-zero asymptotic string tension for color sources in the fundamental representation.²

In a theory with temporary confinement, the simple (and essentially kinematical) motivation for the center vortex mechanism is lost. Then it is not obvious that the center vortex picture, which is motivated by the N-ality properties of the asymptotic string tension, is relevant. The relevance (or irrelevance) of vortices to temporary confinement is a dynamical issue, which we would like to investigate via numerical simulation.

The simplest case to consider is SU(2) gauge-Higgs theory, with the scalar field in the fundamental ($j = 1/2$) representation. Two of our previous articles dealt with this model. The first, written in collaboration with R. Bertle and M. Faber [3], showed that P-vortices percolate when the couplings lie in the temporary confinement region of the phase diagram, and cease to percolate in the Higgs region, where there is no linear potential at all. We also found that center-projected Polyakov lines, in the temporary confinement region, show evidence of color screening by the scalar field. This work did not,

those of SU(N) gauge theory, but the relevant Z_N symmetry is that of the first homotopy group [2].

² In both cases, of course, the asymptotic particle states are color singlets. But this is also true in a Higgs phase, where the condensate screens any external charge. A similar effect occurs in electrodynamics, for electrically charged particles placed in a plasma or a superconductor [1]. One does not normally refer to electric plasmas and superconductors as confining systems; what is going on is charge screening. We believe it is useful to distinguish between this kind of screening of particle charge, and whatever physics lies behind flux tube formation and the linear static quark potential.

¹ In SU(N)/ Z_N pure gauge theory, which has a trivial center and zero asymptotic string tension, vortices and vortex fluctuations are no different from

however, attempt to show that P-vortices in center-projected configurations actually correspond to center vortices in unprojected configurations, as none of our usual tests for that correspondence were employed. A second article, in collaboration with D. Zwanziger [4], considered the spontaneous breaking of a remnant global symmetry, which exists after Coulomb gauge fixing, in the SU(2) gauge-Higgs theory. A confining color Coulomb potential is associated with the unbroken realization of this remnant symmetry, and it was found that remnant symmetry was unbroken in the temporary confinement region, and spontaneously broken in the Higgs region. We did not check, however, whether remnant symmetry breaking and vortex depercolation occur at the same place in the phase diagram (although we assumed this to be true). The reason was that the position of the depercolation transition, found in ref. [3], was determined for a gauge-Higgs theory with variable Higgs modulus, while the position of the remnant symmetry breaking transition, found in ref. [4], was computed in the frozen modulus version of the theory. The present article is intended to fill in these gaps in our two previous articles.

II. CENTER DOMINANCE

We consider a gauge-Higgs theory with a frozen modulus Higgs field. For the SU(2) gauge group, the action can be written as

$$S = \beta \sum_{\text{plaq}} \frac{1}{2} \text{Tr}[UUU^\dagger U^\dagger] + \gamma \sum_{x,\mu} \frac{1}{2} \text{Tr}[\phi^\dagger(x) U_\mu(x) \phi(x + \hat{\mu})] \quad (2.1)$$

where ϕ is SU(2) group-valued. This theory was first studied numerically by Lang et al. [5]; the phase diagram is sketched in Fig. 1. There is a line of first order transitions, but only one thermodynamic phase; any two points in the diagram can be connected by a path which avoids all non-analyticity in the free energy. The absence of a transition completely separating the diagram into a confinement phase and a Higgs phase was demonstrated analytically by Fradkin and Shenker, and Osterweiler and Seiler, in refs. [6]. Nevertheless, below the transition line lies a temporary confinement region, where the static quark potential rises linearly up to some screening distance, while above the line the theory is Higgs-like at all distances, and the static potential is nowhere linear.

We would like to study center dominance inside the temporary confinement region, but close enough to the transition line so that the screening effect of the scalar field is detectable numerically. For this purpose, we compute the expectation value of Polyakov lines at $\beta = 2.2$, on an $L^3 \times 4$ lattice. At $\beta = 2.2$, the first order transition occurs at about $\gamma = 0.84$. The quantity we measure is

$$\langle P \rangle \equiv \left\langle \frac{1}{L^3} \left| \sum_{\mathbf{x}} P(\mathbf{x}) \right| \right\rangle \quad (2.2)$$

where $P(\mathbf{x})$ denotes the Polyakov line passing through the point $\{\mathbf{x}, t = 0\}$. In the case of unbroken center symmetry,

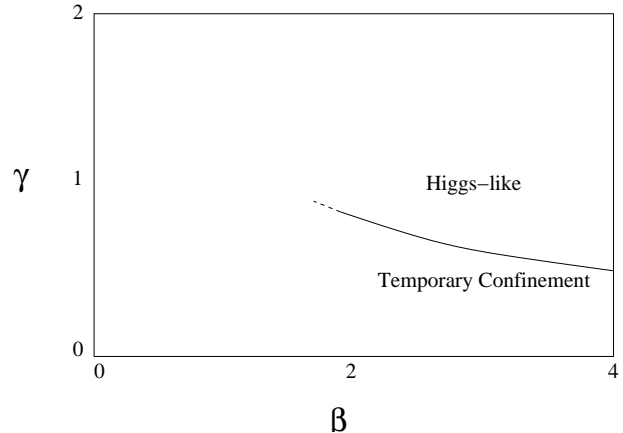


FIG. 1: Schematic phase diagram of the SU(2) gauge-Higgs system. The solid line is a line of first-order phase transitions.

at $\gamma = 0$ and on an $L^3 \times L_T$ lattice, we must find

$$\langle P \rangle \propto \sqrt{\frac{1}{L^3}} \quad (2.3)$$

while for explicitly broken center symmetry ($\gamma \neq 0$) it must be that $\langle P \rangle$ has a non-zero limit at large volume.

Our data for Polyakov lines on the unprojected lattice, at $\beta = 2.2$ and $\gamma = 0, 0.71$, is shown in Fig. 2, for lattice sizes up to $20^3 \times 4$. The straight line is a best fit through the $\gamma = 0$ data, and errorbars for some data points are smaller than the symbol size. It is clear that the $\gamma = 0$ data is consistent with eq. (2.3), and $\langle P \rangle$ extrapolates to zero in the infinite volume limit. At $\gamma = 0.71$ the system is still below the first-order transition line, and in the temporary confinement region. It appears from the data that at this coupling, $\langle P \rangle$ has stabilized (at $L = 14, 16, 20$) to a non-zero value of $\langle P \rangle \approx 0.034(1)$. So at $\beta = 2.2$, $\gamma = 0.71$, color screening of Polyakov lines by the matter field is detectable.

The data at these same couplings, for Polyakov lines on the center projected lattice is displayed in Fig. (3). The center projected data tells exactly the same story as the data on the unprojected lattice: at $\gamma = 0$, Polyakov lines tend to zero at large volumes, while at $\gamma = 0.71$ screening is detected, and the Polyakov lines stabilize at $\langle P \rangle \approx 0.120(4)$. This aspect of center dominance in the SU(2) gauge-Higgs model was previously found in ref. [3], for the variable modulus version of the theory.

We can go on to calculate the correlator of center-projected Polyakov lines $\langle P(x)P(x+R) \rangle$ at $\beta = 2.2$, $\gamma = 0.71$, on a $20^3 \times 4$ lattice. The data is shown in Fig. 4. The dashed line is a best fit to the data, for $R \geq 2$, by the function

$$f(R) = c_0 + c_1 \exp[-4\sigma R] \quad (2.4)$$

From the fit we find $c_0 = 0.0182$, $\sigma = 0.211$. Not surprisingly, c_0 is quite close to the square of the VEV of the Polyakov line in center projection, which is $\langle P_{cp} \rangle = 0.12$ on the $20^3 \times 4$ lattice. In this way we see string-breaking, due to the dynamical matter field, from Polyakov line data on the center-projected lattice.

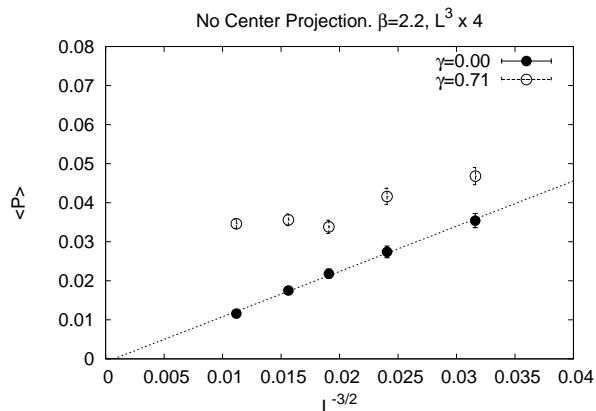


FIG. 2: Polyakov line values, on the unprojected lattice at $\beta = 2.2$, $\gamma = 0$ and $\gamma = 0.71$, on $L^3 \times 4$ lattice volumes with $L = 10, 12, 14, 16, 20$. The straight line is a best fit to the $\gamma = 0$ data.

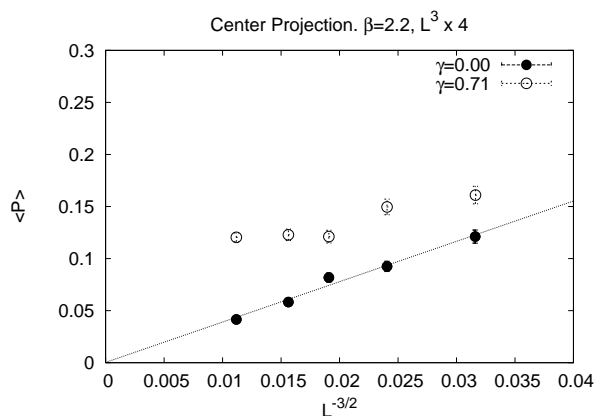


FIG. 3: Same as Fig. 2, for Polyakov lines on the center-projected lattice.

Although the data displayed in the previous graphs makes a good case for center dominance in Polyakov lines in gauge-Higgs theory (which is not a new result), there is still the question of whether P-vortex excitations on the center-projected lattice correlate with gauge-invariant observables on the unprojected lattice. At $\gamma > 0$ global center symmetry is broken, and the 't Hooft loop operator $B(C)$ [7] which creates a thin center vortex would not only raise the action at the loop location, but also on some surface bounded by the vortex loop. The position of this "Dirac surface" is no longer a gauge artifact. We can still identify P-vortices via maximal center gauge fixing and projection, but the correspondence of these P-vortices to center vortices on the unprojected lattice cannot be taken for granted. Our standard test for this correspondence is to see if $W_1(C)/W_0(C) \rightarrow -1$ in the large-loop limit. Here $W_n(C)$ represents a Wilson loop, computed from unprojected link variables, with the restriction that the minimal area of loop C is pierced by n P-vortices on the projected lattice. The result of this test, for spacelike loops on a $20^3 \times 4$ lattice at $\beta = 2.2$, $\gamma = 0.71$ is shown in Fig. 5. It is much like the result found for pure gauge theories, and seems perfectly

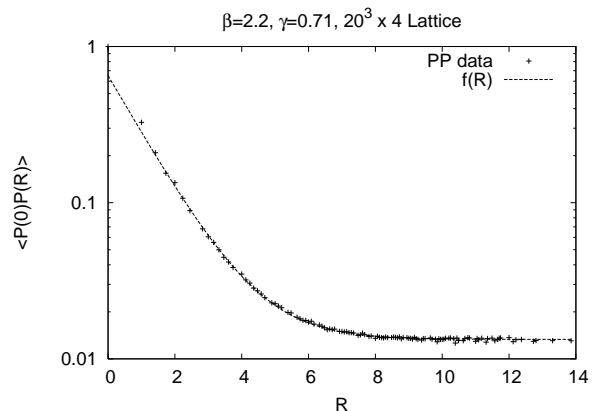


FIG. 4: Polyakov line correlator $\langle P(0)P(R) \rangle$ on the center-projected lattice.

consistent with the assumed correspondence of P-vortices and center vortices.

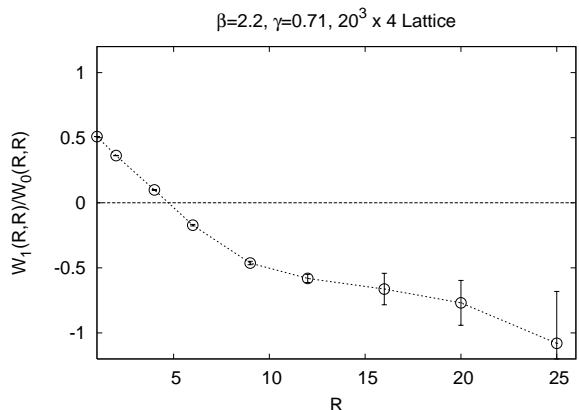


FIG. 5: Ratio of "vortex-limited" Wilson loops. $W_1(C)$ is evaluated for loops pierced by a single P-vortex; $W_0(C)$ is evaluated for loops which are not pierced by any P-vortices.

Finally, we compare the Creutz ratios of projected and unprojected spacelike Wilson loops at $\beta = 2.2$, $\gamma = 0.71$, on the $20^3 \times 4$ lattice, and look for the effect of vortex removal. The relevant data is displayed in Fig. 6. We see that the projected Creutz ratios are constant for any $R > 1$, as in the pure-gauge theory, at roughly $\chi(R,R) \approx 0.21$, and the values for the Creutz ratios on the unprojected lattice also appear to converge towards this value. Note that this value for the asymptotic string tension is consistent with the value obtained from Polyakov line correlators on the projected lattice. The effect of vortex removal is also shown in Fig. 6. Vortices are removed via the de Forcrand-D'Elia prescription [8], which consists of fixing to maximal center gauge, and multiplying each link variable by its center-projected value. This is the vortex-removed ensemble. We see that the Creutz ratios in this ensemble go to zero asymptotically, just as in the pure gauge theory.

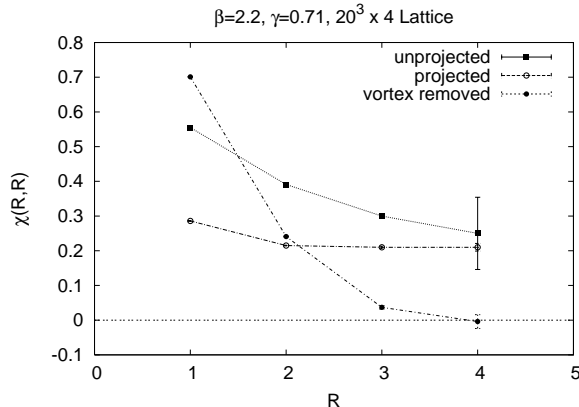


FIG. 6: Creutz ratios in the gauge-Higgs theory for unprojected, center-projected, and vortex-removed lattices.

III. SYMMETRY BREAKING AND VORTEX PERCOLATION

The Fradkin-Shenker theorem [6] assures us that there is no phase transition which completely isolates the temporary confinement region from a Higgs phase; at least, no such transition could be detected by any local order parameter. But what about non-local order parameters? Perhaps thermodynamics is not the ultimate arbiter, and there really exists some qualitative difference between the temporary confinement and Higgs phases, characterized by symmetry-breaking, or by condensation of solitonic objects, which is only detectable via non-local observables. A relevant example is the Ising model in the presence of a small external magnetic field h . In that case the global Z_2 symmetry of the zero-field model is explicitly broken, and there is no thermodynamic transition from an ordered to a disordered state. On the other hand, there is a sharp depercolation transition in the $h > 0$ as well as the $h = 0$ case; the line of such transitions in the temperature- h phase diagram is known as a *Kertész line* [9]. In the gauge-Higgs model the coupling $\gamma > 0$ breaks the global Z_2 symmetry, and it is possible that a sharp vortex depercolation transition could serve to distinguish the temporary confinement and Higgs phases of the theory.

An alternative proposal for distinguishing these phases is associated with symmetry breaking. We know from the Elitzur theorem that a local gauge symmetry can never be spontaneously broken. On the other hand, after Coulomb or Landau gauge fixing there still exists some global remnant of the local symmetry, and these global symmetries *can* be spontaneously broken. So perhaps center vortex depercolation and remnant symmetry breaking define a unique Kertész line, which unambiguously separates the temporary confinement and Higgs phases of the gauge-Higgs model [10]. Another candidate symmetry for distinguishing the two phases, advocated by the Pisa group, is a certain dual (abelian) magnetic symmetry [11]. This approach, in the non-abelian theory, also requires fixing to some gauge.

Since both the identification of vortices, and the definition

of remnant (as well as magnetic) symmetries entails the choice of a gauge, the associated order parameters are non-local (if expressed as gauge-invariant operators), and the Fradkin-Shenker theorem does not rule out non-analytic behavior in such observables. On the other hand, if the transition lines associated with each order parameter do not coincide, then the claim that any of these parameters can be used to “define” confinement, in the absence of a non-vanishing asymptotic string tension, becomes less compelling. In this section we will report on our results for the Kertész lines corresponding to vortex depercolation, and to remnant symmetry breaking in Coulomb gauge.

A. Symmetry Breaking

We begin by reviewing some points made in ref. [4]. First of all, there is a remnant symmetry in “minimal” Coulomb gauge, defined as the gauge which minimizes, on the lattice,

$$R = - \sum_x \sum_{k=1}^3 \text{ReTr}[U_k(x)] \quad (3.1)$$

Fixing to this gauge still allows the following “remnant” gauge transformations which are global in space, but local in time:

$$U_k(\mathbf{x}, t) = g(t) U_k(\mathbf{x}, t) g^\dagger(t) \quad , \quad U_0(\mathbf{x}, t) = g(t) U_0(\mathbf{x}, t) g^\dagger(t+1) \quad (3.2)$$

On any given time slice, this global symmetry can be spontaneously broken, and such breaking implies the absence of a confining color Coulomb potential. The color Coulomb potential can be extracted, at weak couplings, from the correlator of timelike links at a given time, i.e. [4]

$$V_c(R) = - \log \left[\left\langle \frac{1}{2} \text{Tr}[U_0(0, t)] U_0^\dagger(R, t) \right\rangle \right] \quad (3.3)$$

$V_c(R)$ converges to the instantaneous color Coulomb potential in the continuum limit. Asymptotically, this potential is also an upper bound on the static quark potential [12]

$$V(R) \leq V_c(R) \quad (3.4)$$

so that a confining Coulomb potential is a necessary, but not a sufficient, condition for permanent confinement.

The remnant symmetry breaking order parameter Q is expressed in terms of the timelike link variables averaged, at a given time, over spatial volume (L^3)

$$\tilde{U}(t) = \frac{1}{L^3} \sum_{\mathbf{x}} U_0(\mathbf{x}, t) \quad (3.5)$$

If the remnant symmetry (3.2) is unbroken, then the modulus of \tilde{U} should vanish in the infinite volume limit, at any t . We therefore define the order parameter as

$$Q = \frac{1}{L_t} \sum_{t=1}^{L_t} \left\langle \sqrt{\frac{1}{2} \text{Tr}[\tilde{U}(t) \tilde{U}^\dagger(t)]} \right\rangle \quad (3.6)$$

where L_t is the lattice extension in the time direction. Q vanishes in the large volume limit in the unbroken phase, and has a non-zero limit if the remnant symmetry is spontaneously broken.

An exponential falloff in the timelike link correlator implies that the color Coulomb potential rises linearly with separation. In contrast, if remnant symmetry is broken spontaneously, then $V_c(R) \rightarrow \text{constant}$ as $R \rightarrow \infty$. So the existence of an asymptotic Coulomb string tension $\sigma_{coul} > 0$ depends on the unbroken realization of remnant gauge symmetry, and this fact makes the Q order parameter a good candidate for isolating the temporary confinement phase from the Higgs phase.

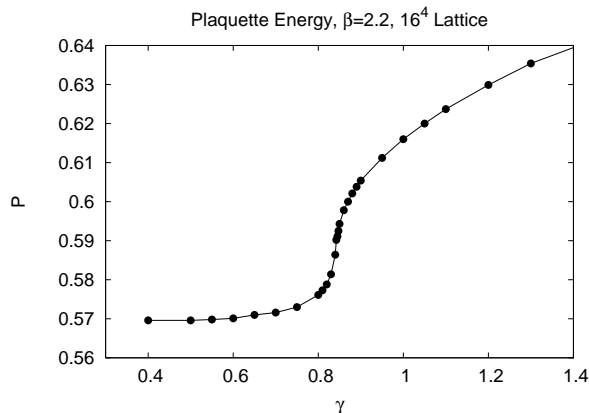


FIG. 7: Plaquequette energy P vs. Higgs coupling γ at $\beta = 2.2$; a weak first-order transition is seen.

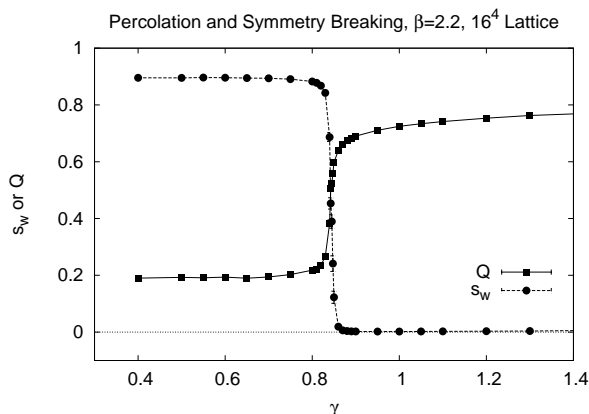


FIG. 8: Data for the remnant symmetry order parameter Q vs. γ , and percolation order parameter s_w vs. γ , at $\beta = 2.2$.

Further support for this view of Q as an order parameter comes from the fact that the Q -transition line in the gauge-Higgs theory coincides with the thermodynamic first-order phase transition line, up to the terminating point of that line of transitions. Like the plaquette energy, the data suggests that Q is discontinuous along the transition line in the infinite volume limit. In Fig. 7 we show the plaquette energy curve, as a function of γ , at $\beta = 2.2$; a weak first-order transition is

visible near $\gamma = 0.84$.³ Fig. 8 shows our data for Q vs. γ , again at $\beta = 2.2$, along with another observable s_w to be discussed shortly. A sudden jump in Q is visible at the same value of γ (within our resolution) that the jump in plaquette energy is observed. The non-zero value of Q below the transition is a finite-size effect; this quantity should vanish on an infinite lattice [4].

As β is reduced, the first-order transition disappears, as seen in the plot of plaquette energy vs. γ at $\beta = 1.2$, shown in Fig. 9. There is still, however, a transition in Q , as seen in Fig. 10. The Q order parameter is not discontinuous in this case, instead, Q increases continuously away from zero (in the infinite volume limit) upon crossing the transition line, at about $\gamma = 1.5$. This behavior is reminiscent of magnetization in a spin system, in the neighborhood of a second order phase transition. In Fig. 10 we show data for both 8^4 and 16^4 lattices, to show the trend to $Q = 0$, at infinite volume, below the transition. We have determined the position of the remnant symmetry-breaking transition line at a range of couplings below $\beta = 2.2$; this is the lower line shown in Fig. 11.⁴

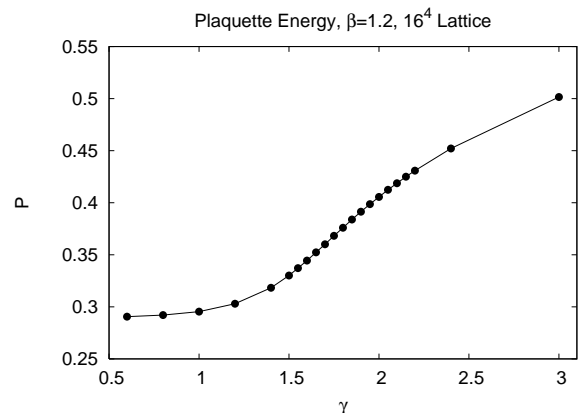


FIG. 9: Plaquequette energy P vs. Higgs coupling γ at $\beta = 1.2$; no transition is evident.

³ We cannot rule out the possibility that this is a very sharp crossover, rather than an actual first-order transition.

⁴ The Q -transition line shown in Fig. 11 differs somewhat in location from the line we reported previously in Fig. 12 of ref. [4]. The calculation of that figure suffered from an unfortunate program error; our current Fig. 11 corrects and replaces it. We note that this program error did not affect the other results reported in ref. [4].

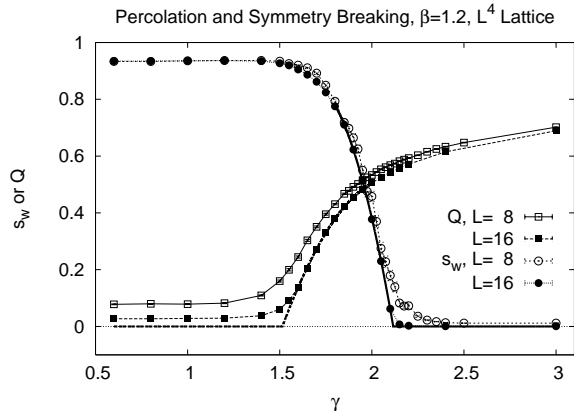


FIG. 10: At $\beta = 1.2$, the remnant symmetry and depercolation transitions occur at different values of γ . Solid lines are presumed extrapolations to infinite volume.

B. Vortex Percolation

We also have a second candidate for the role of order parameter, distinguishing between the temporary confinement and Higgs phases. This is an operator which is sensitive to the vortex percolation-depercolation transition [3], denoted s_w , and defined as follows: Let $f(p)$ be the fraction of the total number N_P of P-plaquettes on the lattice, carried by the P-vortex containing the P-plaquette p . Then s_w is the value of $f(p)$ when averaged over all P-plaquettes. It can be thought of as the fraction of the total number of P-plaquettes on the lattice, contained in the “average” P-vortex. More precisely: let the index $i = 1, 2, \dots, N_v$ denote vortex number, and $i(p)$ specifies the vortex containing the P-plaquette p . Also let n_i denote the total number of P-vortices contained in vortex i . Then

$$s_w \equiv \frac{1}{N_P} \sum_{p=1}^{N_P} \frac{n_{i(p)}}{N_P} = \sum_{i=1}^{N_v} \frac{n_i^2}{N_P^2} \quad (3.7)$$

If all P-plaquettes belong to a single vortex, then $s_w = 1$. In the absence of percolation, the fraction of the total number of P-plaquettes carried by any one vortex vanishes in the infinite volume limit. If a finite fraction of P-plaquettes is carried by a finite number of percolating vortices in the same limit, then $s_w > 0$. The transition from $s_w > 0$ to $s_w = 0$ in the large volume limit identifies the percolation-to-depercolation transition. In ref. [3] we determined the line of depercolation transition in the gauge-Higgs model with variable Higgs modulus; here we report the location (upper line in Fig. 11) in the gauge-Higgs model (2.1), for comparison with the remnant symmetry-breaking line (lower line in Fig. 11). The calculation of s_w requires identifying, on each center-projected lattice configuration, the number of separate P-vortices and the area of each. Our algorithm for doing this is described in detail in the Appendix.

The vortex depercolation transition $s_w \rightarrow 0$, like the Q -transition, coincides with the line of thermodynamic, first-order transitions up to the endpoint of that line. The data for

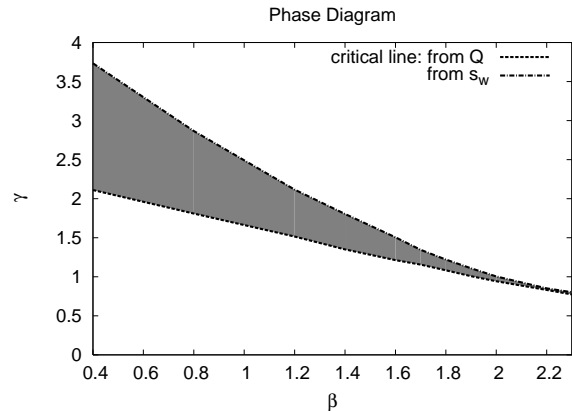


FIG. 11: Transition lines for the remnant symmetry breaking transition (lower line, order parameter Q) and the percolation-depercolation transition (upper line, order parameter s_w). The shaded region is a region of couplings where remnant symmetry is broken, but vortices still percolate. The two transition lines appear to converge at the end-point of the line of first-order thermodynamic transitions.

s_w vs. γ at $\beta = 2.2$ is displayed, together with the Q data, in Fig. 8. However, beyond the first-order transition line, the vortex depercolation and remnant symmetry-breaking transitions no longer coincide, as is evident from our data for Q and s_w at $\beta = 1.2$, displayed in Fig. 10. At this coupling, the Q transition occurs at about $\gamma = 1.5$, while s_w goes to zero at $\gamma = 2.1$.

The transition lines for both remnant-symmetry breaking and depercolation can be compared in Fig. 11 over a range of couplings β , and it is evident that these transition lines do not coincide, contrary to what was assumed implicitly in ref. [4]. There is a region between the two transition lines where vortices percolate, but $\sigma_{coul} = 0$. This is consistent with the notion that vortex percolation is a necessary, but not sufficient, condition for having a confining Coulomb potential, which is itself a necessary, but not sufficient, condition for permanent confinement.

The fact that the vortex and remnant-symmetry transition lines do not coincide tends to support the most straightforward interpretation of the Fradkin-Shenker theorem, namely, that there is no unambiguous distinction between the temporary confinement and Higgs phases. In either region, the large-scale gauge-field fluctuations responsible for disordering Wilson loops are suppressed, and the gauge field due to an external static source falls off exponentially with distance from the source. In this sense the regions are very much alike in the far infrared, and are characterized by charge screening, rather than confining forces.

IV. CONCLUSIONS

There are two conclusions. First, the vortex mechanism for producing a linear potential can work even when the gauge action does not possess a global center symmetry, and the static potential is flat at large distance scales. Thus global center

symmetry is not *necessarily* essential to the vortex mechanism. The same distribution of vortices which produces a linear potential over a finite interval, in temporary confinement theories, can also avoid producing a linear potential at asymptotic distances, as seen in the Polyakov line correlator on the center projected lattice. Of course, the distribution of percolating P-vortices responsible for permanent confinement at $\gamma = 0$, and that responsible for temporary confinement at $\gamma > 0$, must differ qualitatively in some way at large scales. In the latter case, we would expect that vortex piercings of the minimal area of a very large Wilson loop would tend to come in pairs, whose effect on the large loop would cancel. Whether this effect is due to vortices having a branched polymer structure at large scales, or is due to some other distribution, is left for future investigation.

The second conclusion concerns the question of whether it is possible, in a theory without a local order parameter for confinement, to nonetheless distinguish between a “confined” phase and a Higgs phase via some non-local order parameter. We have investigated two reasonable candidates: (i) the Q observable which tests for spontaneous breaking of remnant gauge symmetry in Coulomb gauge, corresponding to the loss of a confining color Coulomb potential, and (ii) the s_w observable, which tests for P-vortex percolation. Both of these observables are closely related to confinement in pure gauge theories; unbroken remnant symmetry is a necessary condition for permanent confinement, and vortex removal removes the confining force. Moreover, both observables have a transition in the gauge-Higgs phase diagram which agrees with the first-order transition line, up to the endpoint of that line. Beyond the first-order transition line, however, we find that the remnant-symmetry breaking and vortex depercolation lines do not coincide, which means that the separation of the gauge-Higgs phase diagram into a “confinement” phase and a Higgs phase is ambiguous. The choice of a particular non-local observable to be an order parameter for confinement is not very compelling, if the only non-analytic behavior seen at the transition is in that particular observable. The fact is that throughout the phase diagram, the gauge-Higgs model at large scales is best described as a color-screening phase. In this model there are no large-scale gauge field fluctuations, characteristic of confinement, which disorder Wilson loops, and the color field due to a static source is screened (as in an electrically charged plasma, or in an electric superconductor), rather than collimated into a flux tube. This observation, together with our numerical result, tends to support the most straightforward reading of the Fradkin-Shenker theorem: There is no essential distinction, in a gauge-Higgs model, between the temporary confinement phase and the Higgs phase.

Acknowledgments

J.G. would like to thank Jan Ambjørn, Phillippe de Forcrand, and Jerzy Jurkiewicz, for helpful discussions. We would also like to thank Roman Bertle, Manfred Faber, and Daniel Zwanziger for collaboration on articles related to the present work. Our research is supported in part by the U.S. Depart-

ment of Energy under Grant No. DE-FG03-92ER40711 (J.G.) and the Slovak Science and Technology Assistance Agency under Contract No. APVT-51-005704 (Š.O.).

APPENDIX

In this appendix we describe our procedure for identifying individual P-vortex surfaces. The basic idea is that two P-vortex plaquettes on the dual lattice which share a common link must belong to the same P-vortex. An ambiguity arises when four or six plaquettes share a link. This could be a self-intersection of a single P-vortex, or an intersection of two or more separate P-vortices. We simply ignore these ambiguous links; they are not used to identify different plaquettes as belonging to the same vortex surface. The algorithm goes as follows:

I. Gauge fix the SU(2) lattice configuration to maximal center gauge, and center project. The center-projected plaquettes have values $z_{\mu\nu}(x) = \pm 1$, where x is the lattice site, and μ, ν specifies the plane of the plaquette.

II. Map the above plaquette variables onto variables onto plaquette variables of the dual lattice

$$z_{\alpha\beta}^D(x + \hat{\mu} + \hat{\nu}) = z_{\mu\nu}(x) \quad (\text{A.1})$$

Although by convention the coordinates of points on the dual lattice are half-integer, we have added a constant vector $(\frac{1}{2}, \frac{1}{2}, \frac{1}{2}, \frac{1}{2})$ to all dual lattice sites in order have integer coordinates on the dual lattice also.

III. Count the number of negative plaquettes on the dual lattice, and assign to each of these a number $n_{\alpha\beta}(x)$ from 1 to A , where A is the total number of negative plaquettes.

IV. Initialize $n_l = 0$. Loop through all of the links of the dual lattice. For each link shared by two *and only two* negative plaquettes, increment n_l , and store the plaquette numbers of the two negative plaquettes in $p(n_l, 1), p(n_l, 2)$. We will refer to such links as “surface-pair” links. Upon completion of the loop over links, set N_l equal to the final value of n_l ; this is the total number of surface-pair links.

V. Initialize the Vortex Number of each negative plaquette, $V(n) = 0$, $n = 1, \dots, A$, and set $n_v = 0$. Now loop through surface-pair links, $n_l = 1, \dots, N_l$. At each such link denote $p_1 = p(n_l, 1), p_2 = p(n_l, 2)$, and then perform the following operation on the vortex numbers:

1. if $V(p_1) = V(p_2) = 0$, increment $n_v \rightarrow n_v + 1$, and set $V(p_1) = V(p_2) = n_v$.
2. if $V(p_1) \neq 0$, $V(p_2) = 0$, set $V(p_2) = V(p_1)$.
3. if $V(p_2) \neq 0$, $V(p_1) = 0$, set $V(p_1) = V(p_2)$.
4. if both $V(p_1), V(p_2)$ are non-zero, and $V(p_1) < V(p_2)$, set $V(p_2) = V(p_1)$.
5. if both $V(p_1), V(p_2)$ are non-zero, and $V(p_2) < V(p_1)$, set $V(p_1) = V(p_2)$.

6. if both $V(p_1)$, $V(p_2)$ are non-zero, and $V(p_1) = V(p_2)$, do nothing.

At the end of looping through the surface-pair links, set $N_v = n_v$.

- VI. Repeat step V, except for the initializations and the setting of N_v . Continue iterating through the surface-pair links until convergence is reached; i.e. there is no further modification of the $\{V(n)\}$.

- VII. Initialize vortex areas $a_n = 0$, $n = 1, \dots, N_v$. Loop through the negative plaquette number $n = 1, \dots, A$. At each plaquette, increment

$$a_{V(n)} = a_{V(n)} + 1 \quad (\text{A.2})$$

- VIII. Eliminate any zero entries in the set of a_n . This can be done by setting $m = 0$ and looping through index $n = 1, \dots, N_v$. If $a_n \neq 0$, increment $m = m + 1$ and set $b_m = a_n$. At the end of the loop, reset $N_v = m$. This is the total number of vortices.

- IX. Calculate s_w .

$$s_w = \sum_{m=1}^{N_v} \left(\frac{b_m}{A} \right)^2 \quad (\text{A.3})$$

-
- [1] J. Greensite, Prog. Part. Nucl. Phys. **51**, 1 (2003) [arXiv: hep-lat/0301023].
- [2] P. de Forcrand and O. Jahn, Nucl. Phys. **B651**, 125 (2003) [arXiv: hep-lat/0211004].
- [3] R. Bertle, M. Faber, J. Greensite, and Š. Olejník, Phys. Rev. **D69**, 014007 (2004) [arXiv: hep-lat/0310057].
- [4] J. Greensite, Š. Olejník, and D. Zwanziger, Phys. Rev. **D69**, 074506 (2004) [arXiv: hep-lat/0401003].
- [5] C. Lang, C. Rebbi, and M. Virasoro, Phys. Lett. **104B**, 294 (1981).
- [6] E. Fradkin and S. Shenker, Phys. Rev. **D19**, 3682 (1979); K. Osterwalder and E. Seiler, Ann. Phys. **110**, 440 (1978).
- [7] G. 't Hooft, Nucl. Phys. **B138**, 1 (1978).
- [8] P. de Forcrand and M. D'Elia, Phys. Rev. Lett. **82**, 4582 (1999) [arXiv: hep-lat/9901020].
- [9] J. Kertész, Physica **A161**, 58 (1989).
- [10] K. Langfeld, in *Strong and Electroweak Matter 2002: Proceedings*, ed. by M. Schmidt (World Scientific, Singapore, 2003), p.302 [arXiv: hep-lat/0212032].
- [11] A. Di Giacomo *et al*, Phys. Rev. **D61**, 034503 (2000) [arXiv: hep-lat/9906024].
- [12] D. Zwanziger, Phys. Rev. Lett. **90**, 102001 (2003) [arXiv: hep-lat/0209105].